

Differential development of high-level visual cortex correlates with category-specific recognition memory

Golijeh Golarai^{1,4}, Dara G Ghahremani^{1,2}, S Whitfield-Gabrieli^{1,3}, Allan Reiss^{4,5}, Jennifer L Eberhardt¹, John D E Gabrieli^{1,3} & Kalanit Grill-Spector^{1,5}

High-level visual cortex in humans includes functionally defined regions that preferentially respond to objects, faces and places. It is unknown how these regions develop and whether their development relates to recognition memory. We used functional magnetic resonance imaging to examine the development of several functionally defined regions including object (lateral occipital complex, LOC)-, face ('fusiform face area', FFA; superior temporal sulcus, STS)- and place ('parahippocampal place area', PPA)-selective cortices in children (ages 7–11), adolescents (12–16) and adults. Right FFA and left PPA volumes were substantially larger in adults than in children. This development occurred by expansion of FFA and PPA into surrounding cortex and was correlated with improved recognition memory for faces and places, respectively. In contrast, LOC and STS volumes and object-recognition memory remained constant across ages. Thus, the ventral stream undergoes a prolonged maturation that varies temporally across functional regions, is determined by brain region rather than stimulus category, and is correlated with the development of category-specific recognition memory.

Functional magnetic resonance imaging (fMRI) studies of human occipitotemporal cortex have revealed a consistent organization that is characterized by regions that preferentially respond to different types of visual stimuli. These regions include the LOC, which responds more to a wide range of objects than to scrambled images¹; a region in the fusiform gyrus, the FFA, which responds more to faces than to other objects or scenes² and is involved in face perception^{3,4} and memory^{5–7}; and a region in the parahippocampal gyrus (PHG), the PPA⁸, which responds more to scenes than to faces or objects and is involved in scene memory^{7,9,10}. Discovery of these functionally defined regions has generated debate about the nature of functional specialization in the ventral visual stream and the role of experience in shaping it^{11–14}. Despite a plethora of research, surprisingly little is known about how these regions develop in the human ventral stream, or how their development relates to proficiency in object, face or scene recognition memory.

Here, we used fMRI to examine the development of the LOC, FFA and PPA from age 7 to young adulthood, relating brain development to recognition-memory ability for objects, faces and scenes. We considered three hypotheses regarding the development of functional regions in the ventral stream. First, these regions may develop early. Accordingly, specialized face processing is evident from early infancy^{15–17}. Second, extensive experience with objects, faces and scenes may be necessary for the development of these cortical regions^{18,19}. Indeed, face-recognition memory reaches adult levels late in development,

around age 16 (refs. 20,21). Thus, the entire ventral stream may approach maturity only in adolescence, in tandem with recognition-memory proficiency. Third, there may be distinct developmental trajectories, in which more category-selective regions such as the FFA and PPA may mature later than less category-selective regions such as the LOC. Furthermore, it is important to determine whether the timing of development is specific to visual categories or cortical regions. For example, do face-selective responses in the STS develop in tandem with the FFA or differentially?

We also asked how the development of these regions manifests in fMRI measurements. One possibility is that the spatial extent of the LOC, FFA and PPA is similar in adults and children. Maturation and experience-dependent gains in perceptual proficiency and memory may be reflected in the response amplitude to objects, faces or scenes. Indeed, adult FFA response amplitudes vary with subjective perception and subsequent memory for faces^{3–7}. A second possibility is that selectivity in the ventral cortex emerges slowly during childhood with accumulated experience. This hypothesis predicts smaller selective regions in children (as compared with adults) that increase in size with age and improved perceptual skills, analogous to the expansion of somatosensory representations with training²². A third possibility is that weaker visual proficiency in children is associated with a larger spatial extent of activation and less efficient processing in children than in adults. Thus, experience may lead to more focal and selective regions for processing specific stimuli in adults, analogous

¹Department of Psychology, Jordan Hall (Bldg. 420), Stanford University, Stanford, California 94305-2130, USA. ²Department of Psychology, Franz Hall, University of California, Los Angeles, Los Angeles, CA 90095-1563, USA. ³Harvard-MIT Division of Health Sciences and Technology (HST) and Department of Brain and Cognitive Sciences, Massachusetts Institute of Technology, 77 Massachusetts Avenue, Building 46-4033, Cambridge, Massachusetts 02139, USA. ⁴Department of Psychiatry and Behavioral Sciences, Stanford University School of Medicine, 401 Quarry, Stanford, California 94305-5722, USA. ⁵Program in Neuroscience, Stanford University, Stanford, California 94305-2130, USA. Correspondence should be addressed to G.G. (ggolarai@psych.stanford.edu).

Received 26 December 2006; accepted 6 February 2007; published online 11 March 2007; doi:10.1038/nn1865

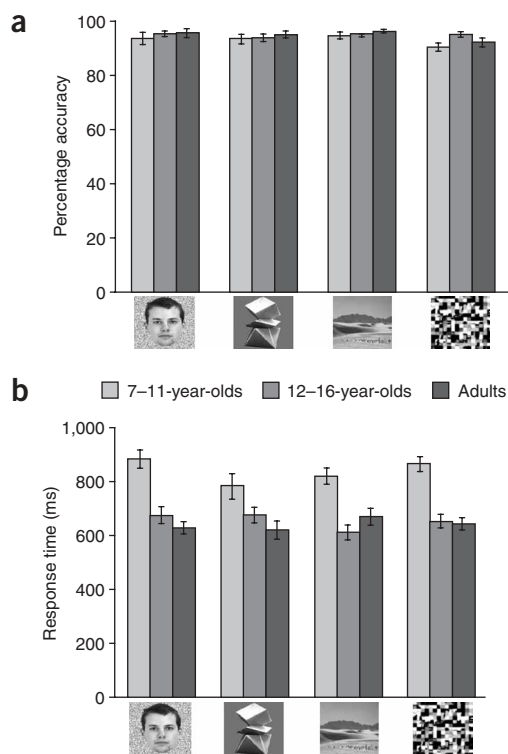


Figure 1 Behavioral data during scan. Accuracy (**a**) and response times (**b**) in a one-back task during the scan, for faces, abstract sculptures, scenes and textures (scrambled objects). Light gray, children ages 7–11; dark gray, children ages 12–16; black, adults. Error bars show s.e.m. for each age group.

infants²⁴, but other studies have reported the absence of face-selective responses (relative to objects or houses) in the fusiform gyri of children 5–8- (ref. 25) and 8–10-years old (ref. 26). These studies did not localize the LOC or PPA or relate cortical maturation to recognition-memory improvements. Furthermore, these studies did not consider possible confounds in comparing activations across age groups—including age-related differences in anatomical size (for example, the fusiform gyrus) or in blood oxygenation level-dependent (BOLD) signals that index neural activity in fMRI.

To characterize the development of cortical specialization for faces, places and objects, we used a combination of fMRI and behavioral methods with children (ages 7–11), adolescents (ages 12–16) and adults. In Experiment 1, we performed fMRI while subjects viewed blocks of faces, scenes, abstract sculptures and textures. For each individual, we functionally defined the FFA, STS, LOC and PPA. We examined the relation between age and the spatial extent, magnitude and selectivity of activations in these regions, while controlling for possible age-related confounds. In Experiment 2, we measured recognition memory for faces, novel objects and scenes in the same subjects outside the scanner, and related recognition-memory performance to the fMRI results.

RESULTS

fMRI of face-, object- and place-selective cortex

In Experiment 1 during fMRI, subjects viewed blocks of images of faces, abstract sculptures, scenes and textures (created by scrambling object images, Fig. 1), and pressed a button when an image was presented twice successively (14% of images, occurring randomly). Accuracy was

to greater activation of primary auditory cortex in non-musicians than in musicians²³.

None of these possibilities has yet been eliminated, as the few imaging studies of occipitotemporal cortex development vary in their findings. A PET study found greater responses to faces than to geometric shapes in the ventral occipitotemporal cortex of 2-month-old

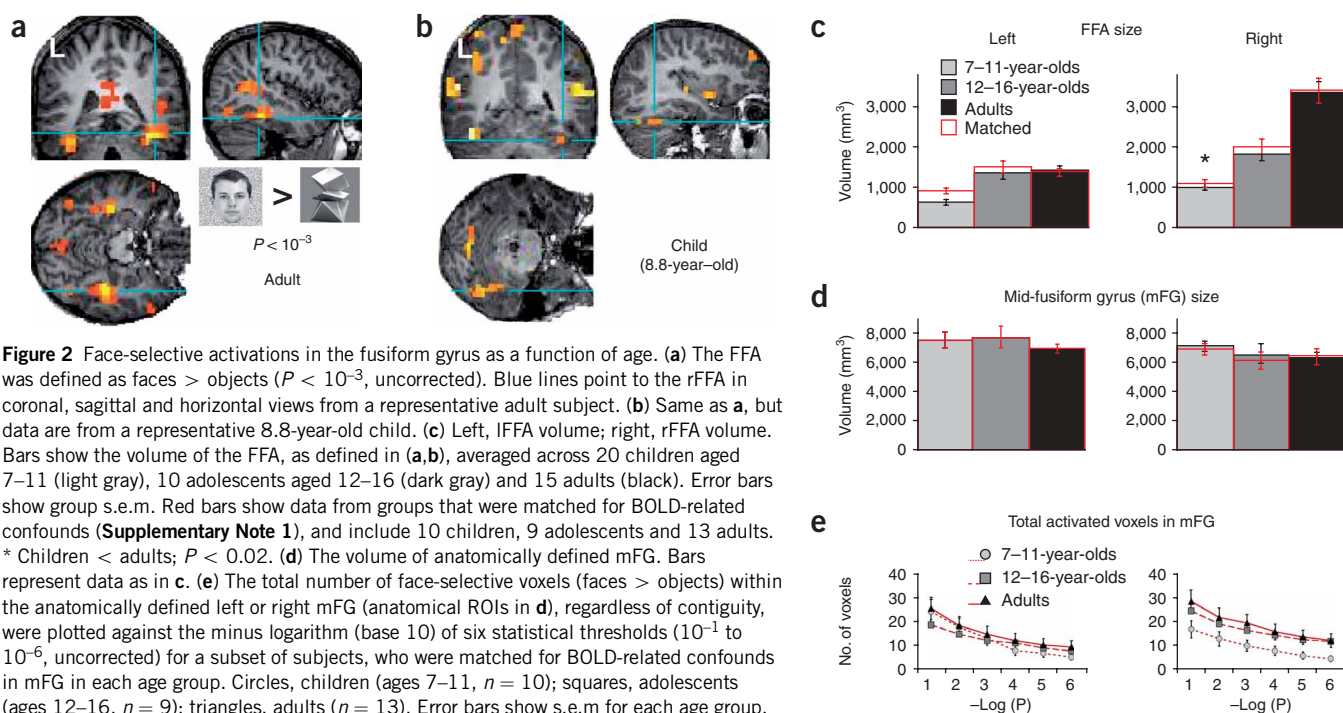
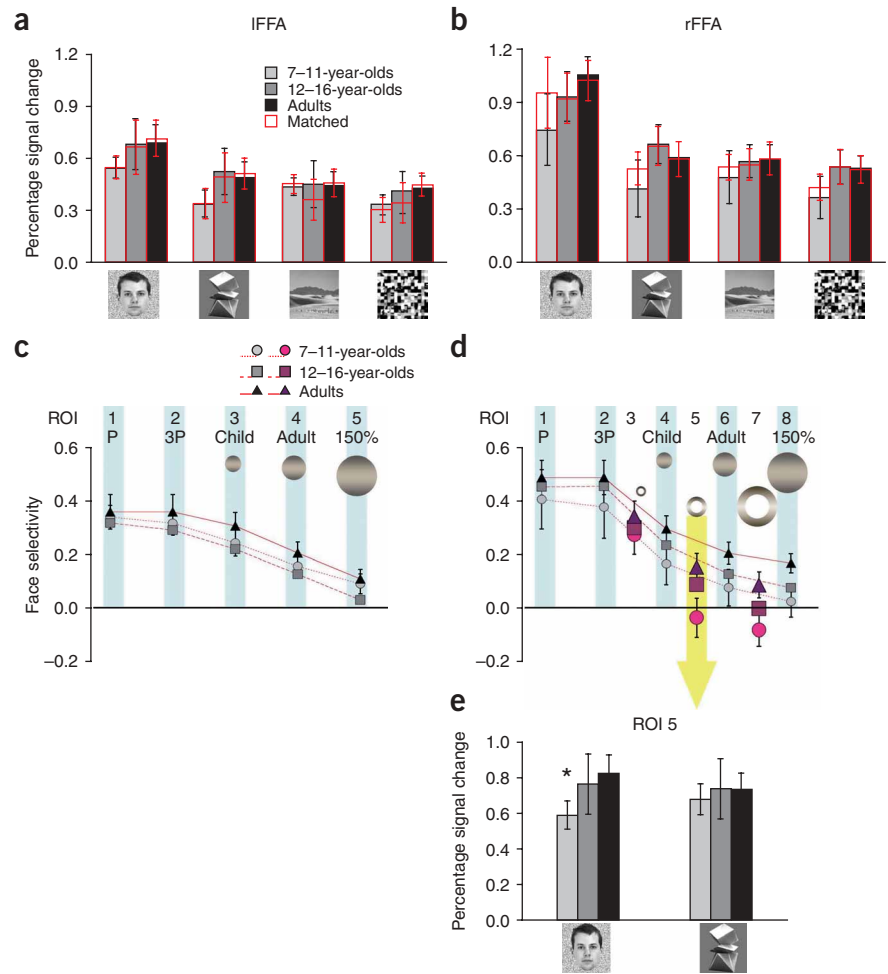


Figure 2 Face-selective activations in the fusiform gyrus as a function of age. (**a**) The FFA was defined as faces > objects ($P < 10^{-3}$, uncorrected). Blue lines point to the rFFA in coronal, sagittal and horizontal views from a representative adult subject. (**b**) Same as **a**, but data are from a representative 8.8-year-old child. (**c**) Left, lFFA volume; right, rFFA volume. Bars show the volume of the FFA, as defined in (**a**,**b**), averaged across 20 children aged 7–11 (light gray), 10 adolescents aged 12–16 (dark gray) and 15 adults (black). Error bars show group s.e.m. Red bars show data from groups that were matched for BOLD-related confounds (Supplementary Note 1), and include 10 children, 9 adolescents and 13 adults. * Children < adults; $P < 0.02$. (**d**) The volume of anatomically defined mFG. Bars represent data as in **c**. (**e**) The total number of face-selective voxels (faces > objects) within the anatomically defined left or right mFG (anatomical ROIs in **d**), regardless of contiguity, were plotted against the minus logarithm (base 10) of six statistical thresholds (10^{-1} to 10^{-6} , uncorrected) for a subset of subjects, who were matched for BOLD-related confounds in mFG in each age group. Circles, children (ages 7–11, $n = 10$); squares, adolescents (ages 12–16, $n = 9$); triangles, adults ($n = 13$). Error bars show s.e.m. for each age group.

Figure 3 BOLD response amplitudes in the FFA and face selectivity. **(a,b)** Percent BOLD signals relative to fixation background for each image category and age-group in the left **(a)** and right **(b)** hemisphere. Bars represent data as in **Figures 1** and **2**. **(c,d)** Average face selectivity (face – object)/(face + object), is plotted for age groups matched for BOLD-related confounds (**Supplementary Note 1**) in the left **(c)** and right hemisphere **(d)**. Positive values along the y-axis indicate preference for faces, negative values preference for objects. Circles, children (ages 7–11); squares, adolescents (ages 12–16); triangles, adults. Error bars show group s.e.m. **(c)** Average face selectivity in a series of concentric ROIs (constant-sized across subjects) in the left hemisphere: P, voxel with the highest *t*-value for faces > objects in mFG (IFFA peak); 3P, similarly, three contiguous voxels with the highest *t*-values. Three spherical ROIs were centered at the IFFA peak in each subject, and sized to match the group average IFFA size in children (Child), adults (Adult) and 150% of the average IFFA size in adults (150%). **(d)** Average face selectivity in a series of concentric spherical ROIs (P, 3P, Child, Adult and 150%) were defined as in **(c)**, but centered on the rFFA peak. Three additional concentric shell ROIs were created as the region in Child excluding 3P (ROI 3), Adult excluding Child (ROI 5) and 150% excluding Adult (ROI 7). Yellow arrow: face selectivity was significantly lower among children ($n = 10$) than among adults ($n = 13$), in the shell representing the penumbral region of the rFFA in children (ROI 5, $P < 0.05$). **(e)** Percent BOLD amplitude for faces and objects versus fixation baseline in the penumbral region of rFFA in children (ROI 5, * children < adults, $P < 0.05$). Data are presented as in **(a)**. Error bars show group s.e.m.



high during this ‘one-back’ task (> 90%) across age groups and image categories (**Fig. 1a**), showing no significant effects of age ($F_{2,42} = 0.29$, $P = 0.74$), age \times image-category interaction ($F_{4,84} = 0.51$, $P = 0.61$) or image category (excluding textures, $F_{2,42} = 0.14$, $P = 0.7$). Response times were longer for children (ages 7–11) than for adolescents (ages 12–16, $t_{28} = 4.6$, $P < 0.0001$) or adults ($t_{33} = 5.67$, $P < 0.0001$; **Fig. 1b**). Response times showed no significant effects of image category ($F_{3,84} = 0.09$, $P = 0.8$) and no interactions between age and image category ($F_{6,126} = 0.91$, $P = 0.4$).

Smaller fusiform face area (FFA) in children than adults

The FFA was defined in each subject as a contiguous cluster of voxels peaking in the fusiform gyrus that responded more to faces than to objects ($P < 10^{-3}$, uncorrected, **Fig. 2a,b**). The FFA was detected more reliably in adults (right FFA: rFFA, 15/15 subjects; left FFA: lFFA, 14/15) and adolescents (rFFA, 10/10; lFFA, 8/10) than in children (rFFA, 17/20; lFFA, 14/20). The rFFA increased in size with age ($F_{2,42} = 5.63$, $P < 0.007$), and was 3.3-fold larger in adults than in children ($t_{33} = 3.34$, $P < 0.002$; **Fig. 2c**). There were nonsignificant trends toward larger rFFA size in adults than in adolescents ($t_{23} = 1.72$, $P = 0.09$, one-tailed) and larger lFFA size in adults compared with children ($t_{33} = 1.98$, $P = 0.07$, one-tailed; **Fig. 2c**).

These results may indicate age-dependent differences in cortical selectivity for faces. Alternatively, they may reflect any combination of the following in children: (i) larger BOLD-related confounds^{27,28}, (ii) smaller anatomical size of the fusiform gyrus, (iii) less clustering of

face selective voxels in the fusiform gyrus and (iv) lower response amplitudes. We examined each of these alternatives.

In each subject, we quantified several BOLD-related confounds: subject motion, BOLD fluctuations during baseline (%cv_BOLD) and residual error (%Res) from the general linear model (GLM, Methods and **Supplementary Note 1** online). Higher BOLD-related confounds in children could potentially compromise the detection of selective voxels using the GLM. In general, BOLD-related confounds were higher in children than in adults, but only %cv_BOLD in the left mid fusiform gyrus (mFG) and subject motion were significantly higher in children than in adults (**Supplementary Table 1** online).

To test whether children’s smaller rFFAs were due to between-group differences in BOLD-related confounds, we compared rFFA size across a subset of subjects that were matched across age groups for these confounds (**Supplementary Note 1** and **Supplementary Table 1**). In this subset of subjects, the rFFA was significantly larger in adults than in children ($t_{21} = 2.41$, $P < 0.02$; **Fig. 2c**). Thus, the smaller rFFA in children was not due to BOLD-related confounds.

There were no significant differences across age groups in whole brain volumes ($F_{2,42} = 1.16$, $P = 0.32$, data not shown) or volume of the right or left mFG (**Fig. 2d**), despite a trend toward larger average mFG size in children than in adults (right mFG: $t_{33} = 1.50$, $P = 0.07$, one-tailed; left mFG: $t_{33} = 1.50$, $P = 0.09$ one-tailed).

We also examined whether children’s smaller rFFAs reflected less clustering of face-selective voxels by counting, regardless of contiguity, the number of voxels in the mFG that activated more strongly for faces

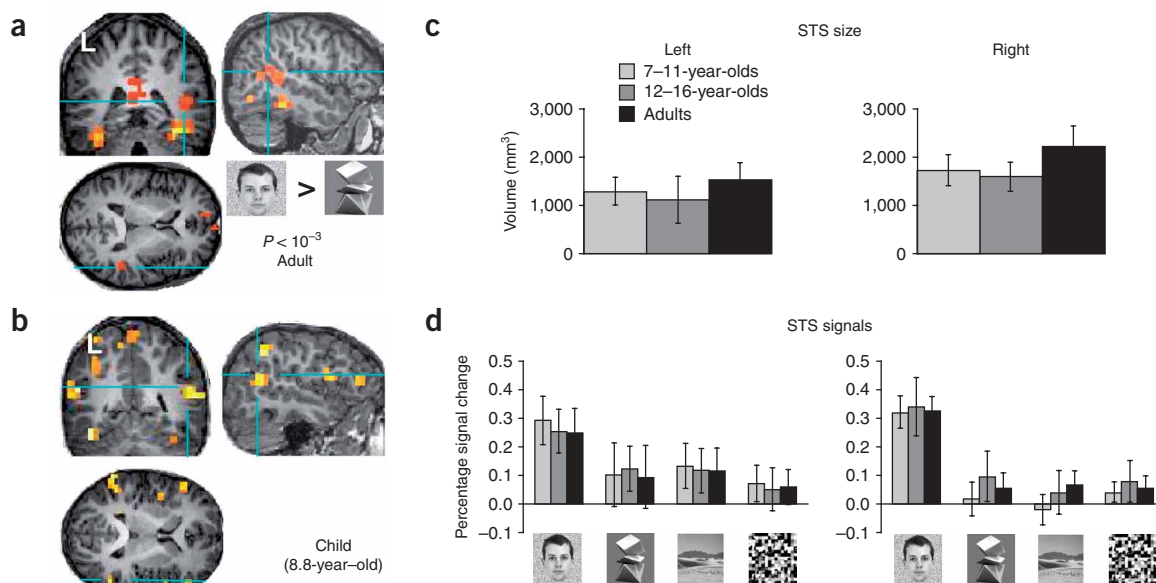


Figure 4 Face-selective activations in the STS as a function of age. **(a)** The STS was defined in the posterior aspect of the superior temporal sulcus, as a cluster of contiguously activated voxels that responded more strongly to faces than to objects ($P < 10^{-3}$, uncorrected). Blue lines point to the rSTS in activation maps from the same representative adult subject as in **Figure 2a**. **(b)** Analogous to **a**, but data are from the same 8.8-year-old child as in **Figure 2b**. **(c)** Average volume of the functionally defined STS (as in **a** and **b**) across children ($n = 20$), adolescents ($n = 10$) and adults ($n = 15$). **(d)** Average BOLD response amplitudes in STS across stimuli and age groups. Bar graphs represent age groups as in **Figure 1**. Error bars show group s.e.m.

than for objects, at six different thresholds ($10^{-6} < P < 10^{-1}$, uncorrected). The number of face-selective voxels in the right mFG was lower in children than in adults at every threshold tested (subjects matched for BOLD-related confounds: $P < 0.05$, corrected for multiple comparisons; **Fig. 2e**; all subjects $P < 0.05$, corrected for multiple comparisons, data not shown).

FFA response amplitudes and selectivity

There were no significant differences in FFA response amplitudes among age groups (rFFA: $F_{2,39} = 1.24$, $P = 0.30$; IFFA: $F_{2,33} = 0.38$, $P = 0.69$) or interaction between age and stimulus type (rFFA: $F_{6,111} = 1.23$, $P = 0.30$; IFFA: $F_{6,96} = 0.87$, $P = 0.43$; **Fig. 3a,b**). Results were similar for subjects matched for BOLD-related confounds (amplitude, rFFA: $F_{2,27} = 0.70$, $P = 0.50$; IFFA: $F_{2,24} = 0.26$, $P = 0.79$; interaction age \times stimulus type, rFFA: $F_{6,78} = 0.09$, $P = 0.91$; IFFA: $F_{6,72} = 0.91$, $P = 0.40$; **Fig. 3a,b**).

Our finding of a smaller rFFA in children predicts a smaller face-selective cortical region surrounding the peak of the rFFA. Accordingly, in subjects matched for BOLD-related confounds, we calculated a face selectivity index (face – object)/(face + object) in an expanding series of regions of interest (ROIs), from the peak FFA voxel to an ROI that was 150% of the adult FFA size. We repeated this analysis by two independent methods, one using constant-sized ROIs (Methods, **Fig. 3c,d**) and another using shape-preserved ROIs (Methods, **Supplementary Fig. 1** online). Face selectivity was significantly lower in children than in adults in the right hemisphere in the ROI matched to the average adult rFFA size (constant-sized: $t_{21} = 1.90$, $P < 0.04$, one-tailed, **Fig. 3d**, ROI 6; shape-preserved: $t_{21} = 2.69$, $P < 0.012$, **Supplementary Fig. 1**). Furthermore, in the region between the two ROIs, one matched in size to the average child rFFA and one to the average adult rFFA, only adults showed face selectivity. Accordingly, face selectivity in this region was significantly lower in children than in adults (constant-sized: $t_{21} = 2.1$, $P < 0.05$; **Fig. 3d**, ROI 5; shape-preserved: $t_{21} = 3.9$,

$P < 0.001$; **Supplementary Fig. 1**). Thus, a region immediately surrounding the nascent rFFA in children is less selective for faces than the corresponding region (falling in the rFFA) in adults.

Children's lower face selectivity in this region was associated with significantly lower responses to faces in children than in adults (constant-sized: $t_{21} = 1.89$, $P < 0.04$, one-tailed, **Fig. 3e**; shape-preserved: $t_{21} = 1.73$, $P < 0.05$, one-tailed, **Supplementary Fig. 1**), but there were no between-group differences in responses to objects ($t_{21} = 0.97$, $P = 0.3$; **Fig. 3e**; shape-preserved: $t_{21} = 0.92$, $P = 0.9$, **Supplementary Fig. 1**). Thus, maturation of the rFFA involves a specific increase in face selectivity and responsiveness in a region immediately surrounding children's rFFA.

No age-related changes in the size of STS or LOC

We defined a face-selective region in each subject's STS (faces > objects, $P < 10^{-3}$, uncorrected; **Fig. 4a,b**). This region was detected in children (right STS: rSTS, 18/20; left STS: lSTS, 15/20), adolescents (rSTS: 8/10; lSTS: 8/10) and adults (rSTS: 14/15; lSTS: 12/15). Unlike the rFFA, there were no significant differences among age groups in the size of the STS face-selective region (rSTS: $F_{2,42} = 0.55$, $P = 0.57$; lSTS: $F_{2,42} = 0.07$, $P = 0.93$, **Fig. 4c**). Similarly, there were no differences in response amplitudes across age groups (rSTS: $F_{3,72} = 0.25$, $P = 0.78$; lSTS: $F_{3,22} = 0.02$, $P = 0.97$, **Fig. 4d**) or interaction between age and stimulus category (rSTS: $F_{3,72} = 0.10$, $P = 0.90$; lSTS: $F_{3,22} = 0.20$, $P = 0.81$). Thus, the smaller rFFA in children is not associated with generally smaller or less responsive face-selective regions.

The LOC was defined in each subject (objects > textures, $P < 10^{-5}$, uncorrected, **Fig. 5a,b**) and was detected in children (right LOC: rLOC, 20/20; left LOC: lLOC, 19/20), adolescents (rLOC: 10/10; lLOC: 9/10) and adults (rLOC: 15/15; lLOC: 15/15). There were no significant differences between groups in LOC size (rLOC: $F_{2,42} = 0.21$, $P = 0.81$; lLOC: $F_{2,42} = 0.07$, $P = 0.93$, **Fig. 5c**) or response amplitudes (rLOC: $F_{2,42} = 0.31$, $P = 0.73$; lLOC: $F_{2,40} = 0.02$, $P = 0.97$;

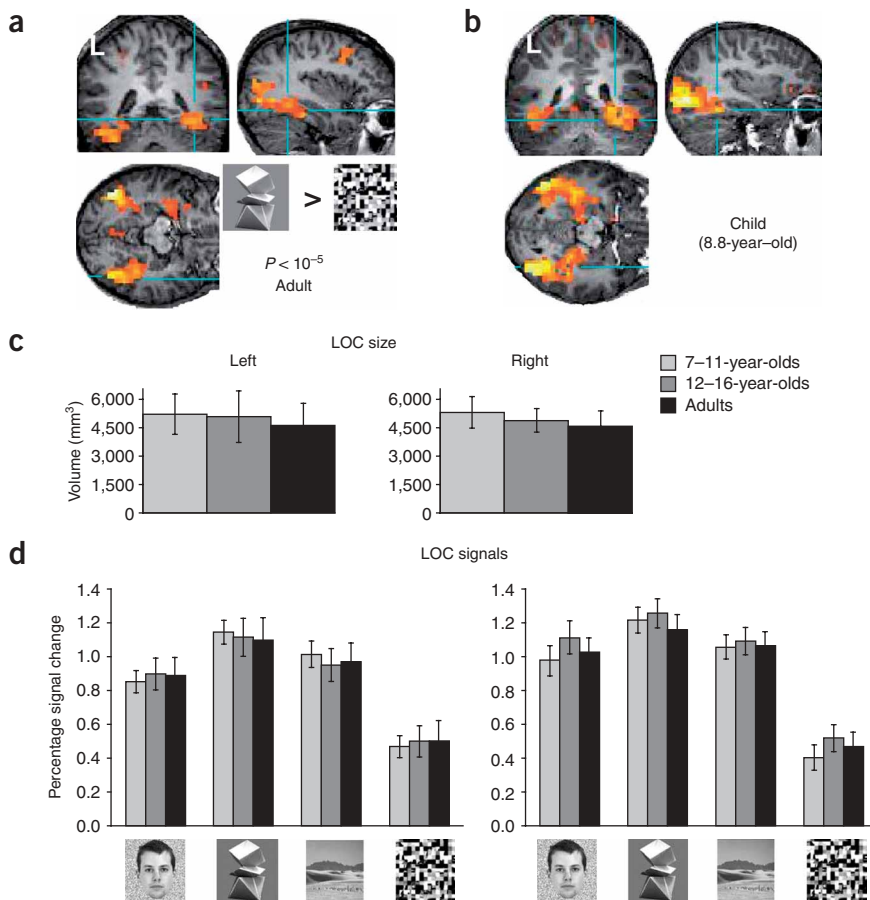


Figure 5 Object-selective activations in the LOC as a function of age. **(a)** The LOC was defined in each lateral occipital cortex, as a cluster of contiguously activated voxels that responded more to objects than textures ($P < 10^{-5}$, uncorrected). Blue lines point to the rLOC from the same representative adult subject as in **Figure 2a**. **(b)** Analogous to **a**, but data are from the same 8.8-year-old child as in **Figure 2b**. **(c)** Average volume of the functionally defined LOC (as in **a** and **b**) across age groups. **(d)** Average BOLD response amplitudes in the LOC for each age group and category. Bar graphs represent age groups as in **Figure 1**. Error bars show group s.e.m.

age \times stimulus category: rLOC: $F_{6,126} = 1.35$, $P = 0.24$; lLOC: $F_{6,120} = 0.36$, $P = 0.90$, **Fig. 5d**). Thus, the LOC reaches adult-like volume and responses by age 7.

Smaller PPA in children than in adults

The PPA was defined in each subject as a cluster of contiguous voxels peaking in the PHG that responded more strongly to places than to objects ($P < 10^{-4}$, uncorrected, **Fig. 6a,b**) and was detected in children (right PPA: rPPA, 17/20; left PPA: lPPA, 16/20), adolescents (rPPA: 10/10; lPPA: 9/10) and adults (rPPA: 15/15; lPPA 13/15). The lPPA increased in size with age ($F_{4,22} = 4.12$, $P < 0.02$) and was significantly larger in adults than in children by a factor of 2.6 ($t_{33} = 2.87$, $P < 0.007$). The size of the lPPA in adolescents was not significantly different from that in children ($t_{28} = 0.95$, $P = 0.34$), but it showed a nonsignificant trend toward smaller size compared with adults ($t_{33} = 1.52$, $P = 0.07$, one-tailed, **Fig. 6c**). The lPPA was also larger in adults than in children, in the subset of subjects matched for BOLD-related confounds ($t_{19} = 2.06$, $P < 0.05$, **Fig. 6c**, **Supplementary Note 1** and **Supplementary Table 2** online). In contrast, rPPA size showed no age effects ($F_{2,42} = 0.52$, $P = 0.6$, **Fig. 6c**). Also, the anatomical volumes of the PHGs were not significantly different across

age groups (right: $F_{2,42} = 1.11$, $P = 0.33$; left: $F_{2,42} = 0.22$, $P = 0.80$, **Fig. 6d**).

Independent of statistical thresholds tested, there were more place-selective voxels within the anatomical boundaries of the left PHG in adults than in children ($t_{33} > 5.0$, $P < 0.0006$, corrected for multiple comparisons; data not shown). This result held for subsets of these groups matched for BOLD-related confounds ($t_{33} > 5.14$, $P < 0.0006$, corrected for multiple comparisons; **Fig. 6e**). Thus, the lPPA undergoes maturation after age 7, increasing in size into adolescence.

PPA response amplitudes and selectivity

Response amplitudes to visual stimuli in the PPA were not different across age groups (rPPA: $F_{2,39} = 0.07$, $P = 0.93$; lPPA: $F_{2,35} = 0.10$, $P = 0.90$; **Fig. 7a,b**). Likewise, there were no significant interactions between age and stimulus category (rPPA: $F_{6,111} = 0.20$, $P = 0.82$; lPPA: $F_{6,99} = 1.03$, $P = 0.37$). Results were similar for subjects matched for BOLD-related confounds (response amplitude, rPPA: $F_{2,30} = 0.07$, $P = 0.93$; lPPA: $F_{2,24} = 0.09$, $P = 0.91$; interaction between age and stimulus, rPPA: $F_{6,84} = 0.09$, $P = 0.91$; lPPA: $F_{6,69} = 1.32$, $P = 0.28$).

In each BOLD-artifact-matched subject, we calculated place selectivity (places – objects)/(places + objects) at the peaks of lPPA and rPPA and in an expanding series of ROIs (**Fig. 7c,d** and **Supplementary Fig. 1**). Consistent with a smaller lPPA size in children, in the region between two ROIs that were respectively matched to the size of the average lPPA in children and adults, place selectivity was significantly lower in children than in adults (constant-sized: $t_{19} = 2.74$, $P < 0.01$, **Fig. 7c**, ROI5; shape-preserved: $t_{19} =$

4.16, $P < 0.0001$ **Supplementary Fig. 1**). In this region, responses to places were lower in children than in adults (constant-sized: $t_{19} = 2.07$, $P < 0.05$, **Fig. 7e**; shape-preserved: $t_{19} = 3.31$, $P < 0.003$, **Supplementary Fig. 1**), but responses to objects were not different (constant-sized: $t_{19} = 0.38$, $P = 0.71$, **Fig. 7e**; shape-preserved: $t_{19} = 0.54$, $P = 0.59$, **Supplementary Fig. 1**). These findings suggest that lPPA maturation involves a specific increase in place responsiveness in the region immediately surrounding children's lPPA.

Recognition memory for faces, objects, and places

The subjects of Experiment 1 later participated in Experiment 2, where they viewed a new set of faces, objects and places in blocks and performed a one-back task (encoding session). Performance (accuracy and response time) was similar to that in Experiment 1 (**Supplementary Note 2** online). Ten to 15 min later, subjects participated in a self-paced unexpected recognition test, serially viewing images that were randomly mixed by category and novelty status ('old', seen during encoding, or 'new', not seen before), and identified them as old or new. For faces, adults' memory was better than children's ($t_{33} = 5.57$, $P < 0.0001$) and adolescents' ($t_{23} = 2.25$, $P < 0.03$), and adolescents' memory was better than children's ($t_{27} = 2.25$, $P < 0.03$, **Fig. 8a**).

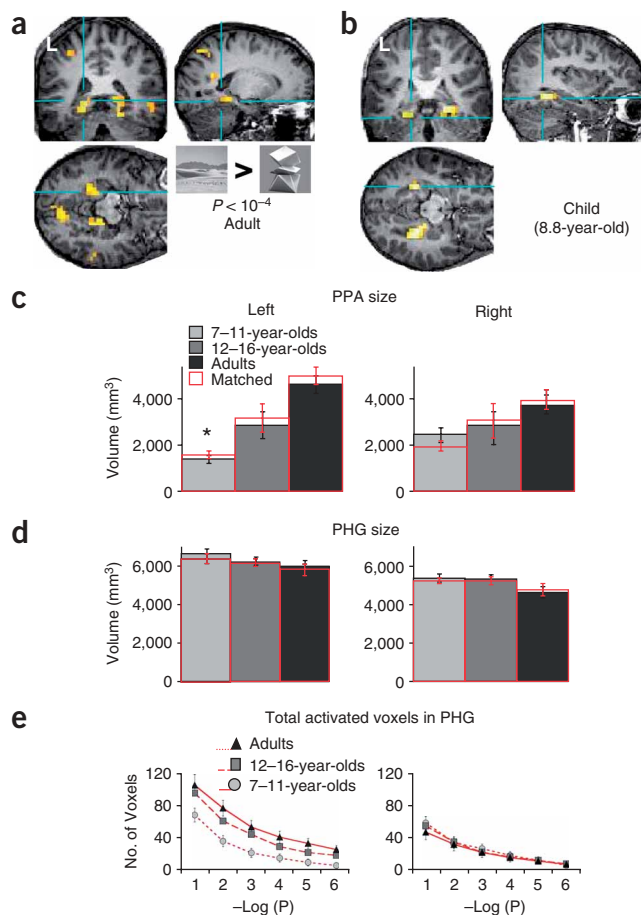


Figure 6 Place-selective activations in the PHG as a function of age. **(a)** The PPA was defined as places > objects ($P < 10^{-4}$ uncorrected). Blue lines point to the IPPA in activation maps from the same representative adult subject as in **Figure 2a**. **(b)** Analogous to **(a)**, but data are from the same 8.8-year-old child as in **Figure 2b**. **(c–e)** Gray scale bars represent age groups as in **Figure 2**. Red bars represent data from groups that were matched for BOLD-related confounds in PHG (**Supplementary Note 1**; right, 10 children, 9 adolescents and 11 adults; left, 10 children, 9 adolescents and 12 adults). Error bars show group s.e.m. **(c)** Left, IPPA volume (* children < adults; $P < 0.05$); right, rPPA volume. **(d)** The volume of anatomically defined PHG in each hemisphere. **(e)** The total number of place-selective voxels (places > objects) within the anatomically defined left and right PHG (anatomical ROIs in **d**), regardless of contiguity, were plotted against the minus logarithm (base 10) of six statistical thresholds (10^{-1} to 10^{-6} , uncorrected) for the subset of subjects who were matched for BOLD-related confounds in the PHG in each age group. Circles, children (ages 7–11, $n = 10$); squares, adolescents (ages 12–16, $n = 9$); triangles, adults ($n = 13$). Error bars show group s.e.m.

that memory improvements for faces and places are related to age-dependent increases in the size of the rFFA and IPPA, respectively, during childhood and adolescence.

DISCUSSION

We found evidence for prolonged development of the IPPA and rFFA, which were about three-fold larger in adults than in children ages 7–11. In children, the nascent rFFA and IPPA were associated with adult-like response amplitudes and selectivity, and were surrounded by functionally immature cortex that did not exhibit face or place selectivity. These age-related increases in rFFA and IPPA volumes were specifically associated with improvements in recognition memory for faces and places, respectively. In contrast, activation volumes for faces in the STS or objects in the LOC remained essentially constant across ages, as did recognition memory for objects. Taken together, these findings suggest that the human ventral stream undergoes a differential maturation process, whereby the LOC develops before the face- or place-selective regions of the rFFA and IPPA, which increased in size at least through age 11, in association with improved category-specific visual recognition memory.

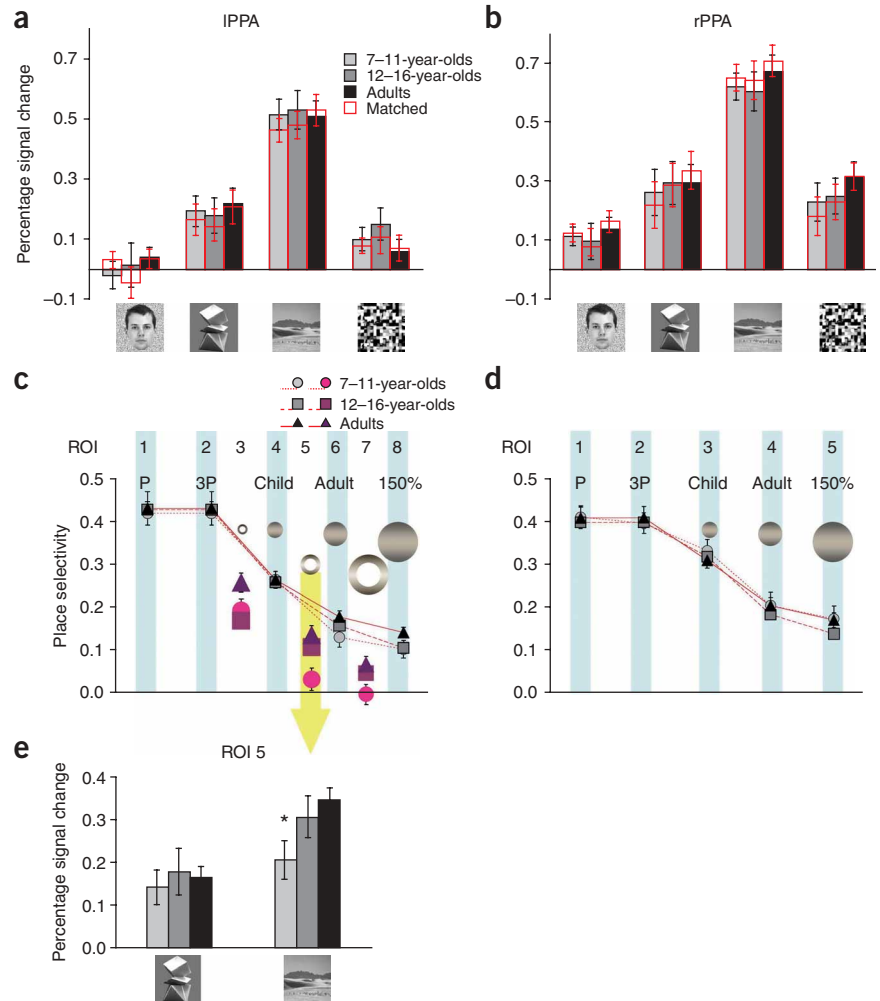
Our controls indicated that the age-related increases in the size of the rFFA and IPPA were not due to possible confounds of developmental functional neuroimaging^{27,28}. First, results were not due to differences in behavioral performance during scanning. Children's response accuracy was adult-like and their longer response times did not vary across categories during the one-back task. Second, results were not driven by potential age-dependent differences in brain size, shape or precise location of functional regions, as ROIs were defined in each subject without spatial normalization. Third, results remained similar in a subset of children and adults who were matched for several factors that could account for age-related confounds, such as subject motion, BOLD signal variability and goodness-of-fit of the GLM. Fourth, our results did not reflect age-related differences in anatomical volumes because mid-fusiform and parahippocampal volumes remained unchanged across age groups. Finally, our results were robust across a wide range of thresholds on statistical maps.

Overall, our data may explain previous failures to detect the FFA in 5–8-year-olds²⁵ or 8–10-year-olds²⁶ using normalized group analyses and concur with a report of smaller FFA in children (and delayed maturation relative to LOC) during viewing of movie segments of faces, places and common objects (K.S. Scherf *et al.*, *Soc. Cog. Neurosci. Abstr. E138* 2006). Developmental expansions of functional regions were correlated with developmental changes in visual recognition memory.

Similarly, for places, adults' memory was better than children's ($t_{33} = 4.84$, $P < 0.0001$), showing a trend toward better memory relative to adolescents' ($t_{23} = 1.48$, $P = 0.07$), and adolescents' memory was better than children's ($t_{27} = 2.65$, $P < 0.01$). There were no effects of age on memory for objects ($F_{2,42} = 0.49$, $P = 0.6$).

We asked whether memory performance for faces, objects or places was specifically related to the size of particular cortical regions in the ventral stream. We regressed memory performance for each category (face, place and object) against multiple factors of age, FFA, PPA, STS and LOC size. Face-recognition memory was significantly correlated with age ($r = 0.47$, $P < 0.001$) and rFFA size ($r = 0.31$, $P < 0.035$), but not with the size of other ROIs tested (P values > 0.18). Face-recognition memory and rFFA size were significantly correlated in children ($r = 0.49$, $P < 0.03$, $n = 20$, **Fig. 8b**) and adolescents ($r = 0.61$, $P < 0.03$, one-tailed, $n = 10$), but not in adults ($r = 0.32$, $P < 0.24$, $n = 15$), perhaps as a result of a more restricted range of memory performance among the latter group. Place-recognition memory was significantly correlated with age ($r = 0.45$, $P < 0.001$) and the size of the IPPA ($r = 0.44$, $P < 0.001$), but not with the size of other ROIs tested ($P > 0.3$). Place-recognition memory and IPPA size were significantly correlated in all groups (children $r = 0.79$, $P < 0.0001$, $n = 20$, adolescents $r = 0.80$, $P < 0.009$, $n = 10$, adults $r = 0.59$, $P < 0.03$, $n = 15$, **Fig. 8c**). Object-recognition memory was not significantly correlated with age, with the size of the LOC (**Fig. 8d,e**) or with the size of any ROI tested ($P > 0.4$). A complementary analysis showed that rFFA size correlated with face but not place and object memory, and IPPA size correlated with place but not object and face memory (**Supplementary Note 2**). These findings support the hypothesis

Figure 7 BOLD response amplitudes in the PPA and place selectivity. **(a,b)** Percent BOLD signals relative to fixation background for each image category and age-group in the left **(a)** and right **(b)** hemisphere. **(c,d)** Average place selectivity, (place – object)/(place + object), in concentric ROIs (constant-sized across subjects) is plotted for age groups matched for BOLD-related confounds in the PHG (**Supplementary Note 1**) in the left **(c)** and right hemisphere **(d)**. **(c)** Average place selectivity in a series of concentric ROIs (constant-sized across subjects, ROI 1 to 8) centered at the IPPA peak in each subject. Spherical ROIs were sized to match the group averaged IPPA size in children (Child) and in adults (Adult) and 150% of the average IPPA size in adults (150%). Shell ROIs were defined as the region in Child excluding 3P (ROI 3), Adult excluding Child (ROI 5) and 150% excluding Adult (ROI 7). Yellow arrow: place selectivity was significantly lower among children ($n = 10$) than among adults ($n = 12$), in the shell representing the penumbral region of the IPPA in children (ROI 5, $P < 0.01$). **(d)** Average place selectivity in a series of concentric ROIs (ROI 1 to 5) as in **(c)**, but centered at the peak of the rPPA in individual subjects and relative to the average size of the rPPA in children and adults. Place selectivity was not statistically different among the age groups, for any of these ROIs in rPPA. **(e)** Average BOLD response amplitudes to places and objects within the ROI representing the penumbral region of the IPPA in children (ROI 5, children < adults, $*P < 0.05$). Error bars show group s.e.m.



Children performed similarly to adults in recognition-memory accuracy for objects, but showed lower accuracy for faces and places than adults. Critically, between age groups, accuracy for faces and for places correlated specifically with the volume of rFFA and IPPA, respectively. It is well established that children reach adult-like proficiency in face-recognition memory around age 16 (refs. 20,21). Accordingly, adults outperformed adolescents, ages 12–16, in our study. However, we show here for the first time that memory for places also undergoes a prolonged development. The apparent coupling between the expansion of category-specific visual cortices and recognition-memory abilities warrants further examination for other visual and mnemonic categories^{29–31} and other tasks. For example, FFA responses, in particular, have been related to face detection and identification^{4,32}, but little is known about the development of these perceptual abilities or their relation to brain function in children.

Prolonged development of rFFA and IPPA manifested as an expansion in the spatial extent of these regions. Children's rFFA was a third of adult size, but still evident in 85% of child subjects. Further, regardless of whether we used a clustering criterion, we found that children, compared with adults, had fewer face- and place-preferring voxels in the fusiform and PHG, respectively, rather than more spatially scattered activations for these stimuli.

In all functionally defined regions, whether smaller than or equal to adult size, children showed adult-like response magnitudes and selectivity. The smaller rFFA and IPPA in children were surrounded by cortices with adult-like responses to objects, but no selectivity for faces or places, respectively. Thus, our findings suggest that prolonged FFA and PPA development is associated with an expansion of a stimulus-

selective region, by means of increased category-specific response amplitudes in an immature penumbral region.

The mechanisms underlying this expansion are unknown, but may include regional increases in the number and/or sharper tuning of face- or place-responsive neurons³³. Indeed, electrophysiological recordings in monkeys show that training to recognize novel visual stimuli increases the number of neurons responsive to the learned category in the anterior inferotemporal cortex of monkeys over periods of several months to years³⁴. Thus, with accumulated experience, more neurons may code for the preferred category in the penumbral regions of the rFFA and IPPA, leading to improved proficiency in face and place recognition, respectively.

Maturation of FFA and PPA regions may involve a variety of mechanisms. For example, there may be age-dependent variations in face and place viewing patterns. It has previously been found³⁵ that atypical patterns of fixation on face parts in autism were associated with lower levels of fusiform gyrus responses to faces. There is currently no evidence indicative of differences between children and adults in patterns of fixation³⁶ or face or place viewing. However, our findings suggest the usefulness of future developmental studies of face and place viewing patterns and their relationship to FFA and PPA responses. Additional factors that may modulate FFA responses include the level of expertise with stimuli^{18,19}, stimulus similarity³⁷ and age-of-the-face stimuli (as there is evidence for a small but observable bias for better recognition of own-age faces, especially among adults³⁸). Future studies

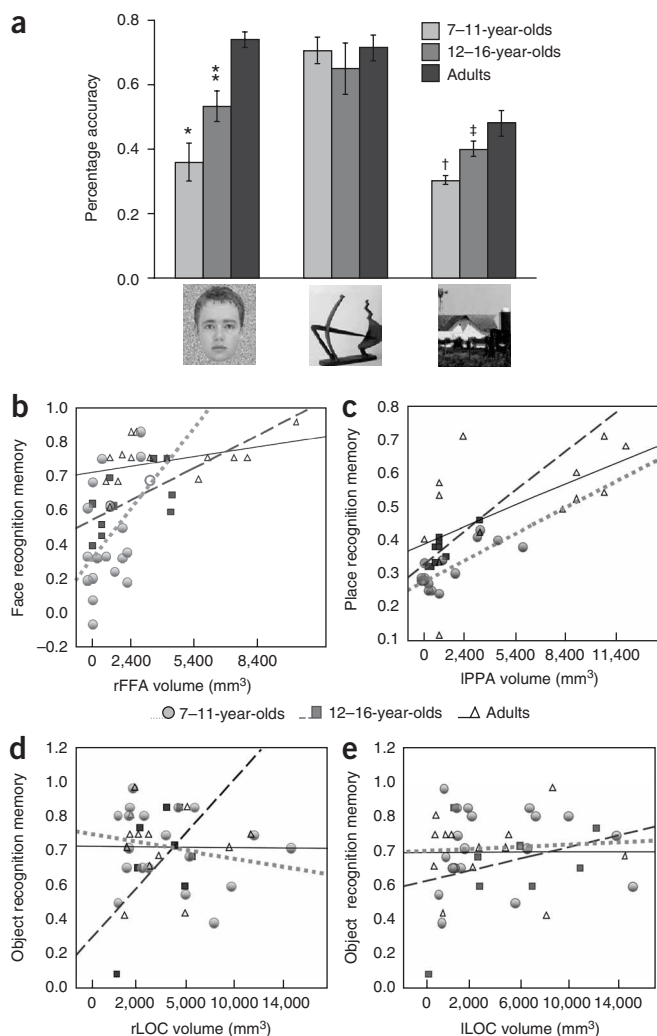


Figure 8 Performance of different age groups on an independent recognition-memory test for faces, abstract sculptures and places. **(a)** Recognition accuracy (percent accuracy = (hit – false alarm)/total) for faces, places and objects. Face-recognition-memory performance in adults was higher than children's ($*P < 0.0001$) or adolescents' ($**P < 0.03$). Adolescents' face-recognition-memory performance was higher than children's ($**P < 0.03$). Place-recognition-memory performance in adults was higher than children's ($\dagger P < 0.0001$). Adolescents' memory for places was higher than children's ($\ddagger P < 0.01$). Error bars show group s.e.m. **(b)** Correlations for face-recognition memory and rFFA size are shown for each age group. **(c)** Correlations for place-recognition memory and IPPA size are shown for each age group. **(d,e)** Correlations for object-recognition memory and right or left LOC size are shown for each age group.

supported by rFFA and IPPA take longer to mature than those supported by LOC or STS. FFA and PPA have been implicated in holistic processing^{13,19,43}, which is disrupted by inversion of faces⁴⁴ and places⁴³. Acquiring the capacity for holistic representation of a category may take longer than for feature-based representations that may occur in LOC^{45,46}. Second, rFFA and IPPA may retain more plasticity (even in adulthood) than LOC and STS, as at least FFA responses are modulated in adults by their level of expertise^{18,19}. Third, prior experience with stimuli may affect brain regions and behavior differentially, depending on stimulus category. Although all study stimuli were novel, our subjects were likely to have had more prior experience with faces than abstract sculptures. However, prior experience had little effect on LOC responses or on recognition memory in adults, which was equal for faces and objects (but worse for places). Using stimuli that are varied systematically for similarity³⁷ and participants' prior experience^{18,19,29} may further reveal the role of experience in ventral stream activations and recognition-memory performance.

Our finding of differential development across the ventral stream speaks to developmental theories of high-level vision. First, it is evident that at least some areas have a prolonged development that is not completed in early childhood. Second, our findings indicate that the entire visual ventral stream is not maturing at the same rate. Rather, there are different temporal trajectories toward reaching adult-like volumes of fMRI activation, and these trajectories seem to relate more to brain regions rather than to stimulus categories. Another implication of our data is that experience may have a more extended role in shaping the brain organization of perception and memory for faces and places than for objects. Finally, our findings form a framework for a better understanding of the normal development of high-level visual cortex in children and the neural basis of developmental disorders of face processing.

METHODS

Subjects. Healthy children ages 7–11 ($N = 23$, 13 females), adolescents ages 12–16 ($N = 10$, 5 females) and adults ages 18–35 ($N = 17$, 8 females) participated in Experiment 1 (in scanner) and Experiment 2 (outside scanner). Subjects were right handed with normal or corrected vision and without any past or current neurological or psychiatric conditions, or structural brain abnormalities. Children and adolescents were recruited from the Palo Alto school district through advertisements in school newspapers and contact with parents, evaluated with a battery of cognitive and perceptual tests, and included if their performance was within the age-appropriate normal range. Adult subjects were Stanford University students. Informed consent was obtained according to the requirements of the Panel on Human Subjects in Medical Research at Stanford University. All subjects were acclimated to the scanning environment by participating (on a previous day) in an anatomical scanning session (unrelated to the fMRI experiments reported here).

Experiment 1. Stimuli. During fMRI, subjects viewed 60 gray-scale photographic images of each of the following five categories: faces, abstract sculptures

will be instrumental in examining the role of these factors in explaining the development of FFA responses.

The differential time course of development across high-level visual cortex varied across regions, not just perceptual categories. In children, there was a dissociation between the smaller volume of rFFA and the adult-like volumes of face-selective regions in IFFA and bilateral STS. Similarly, we found a dissociation between the smaller volume of IPPA in children and their adult-like volume of rPPA. The slower growth of the rFFA is noteworthy, as there is evidence suggesting that face processing is right-hemisphere dominant^{39–41}. Consistent with previous fMRI studies, the rFFA in adults was more reliably found and two-fold larger than the IFFA. Thus, the slower development of rFFA may be a limiting factor in the maturation of face perception and memory. In contrast, the more rapid maturation of STS relative to rFFA suggests that functions associated with the STS (such as processing of gaze direction and other socially communicative cues⁴²) may develop more rapidly than functions associated with the FFA (such as face recognition).

The PPA's unexpected asymmetry of development is more difficult to interpret, as currently there is no evidence for hemispheric specialization for place perception. Thus, this finding awaits, and may eventually contribute to, a better understanding of PPA's functional asymmetry.

The reasons for different rates of development in high-level visual cortex are unknown. One possibility is that the types of representations

(objects), indoor and outdoor scenes, and textures (created by randomly scrambling object pictures into 225, 8×8 -pixel squares; **Fig. 1a**). All faces were of European-American males in a frontal view, displaying a neutral expression with no eyeglasses or jewelry. We chose abstract sculptures, rather than common objects, as exemplars of the object category to selectively activate the LOC^{1,47} and to equate stimulus novelty and the level of verbal labeling across categories.

Behavioral task during fMRI. Each stimulus type was presented during five pseudo-randomly ordered blocks. Blocks were 14 s long followed by 14 s of fixation. Images were presented at 1-s intervals, each for 970 ms, followed by a 30-ms fixation baseline. Each image was presented only once, except for two random images per block, which were presented twice in succession (14% of presentations). Subjects were instructed to fixate on each image and press a button using their right index finger whenever they detected identical images appearing successively (a one-back task).

Images were projected onto a mirror mounted on the MRI coil (visual angle $\sim 15^\circ$). Images were presented and responses were recorded via a Macintosh G3 computer using Matlab 5.0 (Mathworks) and Psychtoolbox extensions (<http://www.psychtoolbox.org>).

Behavioral responses. Percent accuracy during the one-back task was calculated for each subject separately for each image category as $100\% \times (\text{hits/number of repeated images}) - (\text{false alarms/number of nonrepeated images})$. Response times during the one-back task were calculated for each image category as the median time for correct responses for each subject.

Scanning. Brain imaging was performed on a 3-Tesla whole-body General Electric Signa MRI scanner (General Electric) at the Lucas Imaging Center, Stanford University, equipped with a quadrature birdcage head coil. Subjects were instructed to relax and stay still. We placed ample padding around each subject's head and also made use of a bite bar (made of Impression Compound Type I, Kerr Corporation) to stabilize the head position and reduce motion-related artifacts during the scans. First, a high-resolution three-dimensional Fast SPGR anatomical scan (124 sagittal slices, $0.938 \text{ mm} \times 0.938 \text{ mm}$, 1.5-mm slice thickness, 256×256 image matrix) of the whole brain was obtained. Next, a T2-weighted fast spin echo in-plane with a slice prescription identical to that of the functional scan was acquired. Functional images were obtained using a T2*-sensitive gradient echo spiral-in/out pulse sequence using BOLD contrast⁴⁸. Full brain volumes were imaged using 21 slices (4 mm thick plus 1 mm skip), oriented parallel to the line connecting the anterior and posterior commissures. Brain volume images were acquired continuously with TR 1,400 ms, TE 30 ms, flip angle 70° , field of view 240 mm, $3.75 \text{ mm} \times 3.75 \text{ mm}$ in-plane resolution and 64×64 image matrix. Data acquisition time for Experiment 1 was approximately 14 min.

Preprocessing. The first ten functional volumes were discarded to allow for T1 equilibration. Functional images were 'median-filtered' to reduce transient BOLD artifacts using an in-house algorithm, realigned to correct for motion, spatially smoothed using a 6 mm full-width-half-maximum kernel, and temporally filtered (high-pass, 56 s cut-off) using the Statistical Parametric Map software package (SPM2, Wellcome Department of Cognitive Neurology). Data were not spatially normalized. Data from three children and two adults were not used for further analysis due to excessive motion ($> 2 \text{ mm}$).

General linear model. For each subject, statistical modeling was performed using a GLM in SPM2 on preprocessed functional images, excluding images with an average BOLD signal exceeding 2 s.d. from the mean. In a given subject, the number of excluded images did not exceed 15 out of 600 (2.5% of the time series).

The resulting *t*-maps corresponding to the contrast and threshold of interest (uncorrected for multiple comparisons) were overlaid on the individual's high-resolution T1 image (which was co-registered to the mean motion-corrected and non-smoothed functional image).

Whole brain volumes. Brain volume analyses were performed using the FMRIB Software Library (FSL, <http://www.fmrib.ox.ac.uk/fsl/>). For each subject, non-brain parts were automatically removed using FMRIB's Brain Extraction Tool⁴⁹. Volumes were estimated by counting nonzero voxels within these images.

ROI creation. Five types of ROIs (that is, anatomical, functional-cluster, functional-noncluster, constant-sized and shape-preserved) were created for each subject.

1. Anatomical ROIs of the right and left mid-fusiform and PHGs were hand drawn (MRICro, <http://www.mricro.com>) for each subject, based on their non-normalized high-resolution anatomical image (SPGR). All of the anatomical ROIs were drawn by a well-trained person who was blind to the identity and age of the brains. The anatomical ROIs of the mFG in all subjects included the fusiform gyrus between the occipito-temporal sulcus, and the lateral bank of the collateral sulcus. The anterior-to-posterior extent of the fusiform gyrus was limited to a region between the posterior edge of the amygdala and the midpoint along the calcarine fissure. The anatomical ROIs of the PHG included a region between the medial bank of the collateral sulcus and the hippocampus, and posteriorly, the isthmus. The anteroposterior extent of the ROI was limited by the posterior edge of entorhinal and anterior calcarine sulcus⁵⁰.

2. Functional (cluster) ROIs for FFA, STS, LOC and PPA were defined in each subject as contiguous suprathreshold voxels with the following properties and locations: FFA, faces $>$ abstract objects ($P < 10^{-3}$) peaking in the mFG; STS, faces $>$ abstract objects ($P < 10^{-3}$) in the superior temporal sulcus; LOC, abstract objects $>$ scrambled ($P < 10^{-5}$) in the posterior and lateral aspects of the occipital cortex; PPA, places $>$ abstract objects ($P < 10^{-4}$) peaking in the PHG. The statistical thresholds we used were based on conventional definitions.

3. Functional (noncluster) ROIs included all suprathreshold voxels (regardless of clustering) within the relevant anatomical ROI (the mFG for FFA and the PHG for the PPA) for the contrast of interest (that is, faces $>$ abstract objects for FFA, places $>$ abstract objects for PPA) at six different statistical thresholds ($10^{-1} < P < 10^{-6}$). Thresholds were based on whole brain analysis, uncorrected for multiple comparisons.

4. Constant-sized ROIs included all voxels (whether or not they exceeded a statistical threshold) within a predefined volume in the vicinity of the FFA or the PPA. For the FFA, spherical ROIs were all centered at the individual's FFA peak (faces $>$ objects, $P < 10^{-3}$, see **Fig. 3**). When no FFA was found, spherical ROIs were centered at the subject's most face-responsive voxel (highest *t*-value for faces $>$ textures) in the mid-fusiform gyrus. For each hemisphere, the size of these ROIs were fixed to include the volume defining (i) the peak voxel (P), (ii) three contiguous voxels with the highest *t*-values (3P), (iii) the average size of the FFA in the children's group (Child), (iv) the average size of the FFA in the adult group (Adult) and (v) a region 150% of the average FFA in adults (150%). A series of concentric shells were also defined as the regions between spherical ROIs (ROI 3: voxels of Child excluding 3P voxels; ROI 5: Adult excluding Child; ROI 7: %150 excluding Adult). For the PPA, spherical and shell ROIs were similarly created and centered at the PPA peak, or in the cases where no PPA was found, the most place-selective voxel (highest *t*-value for places $>$ scrambled) in the PHG in each subject and hemisphere (**Fig. 7**). The sizes of the PPA-peak centered spherical ROIs were based on the group averaged PPA size in adults or children in each hemisphere.

5. Shape-preserved ROIs were created by growing or shrinking subject-specific functional ROIs. This involved adding or removing voxels starting from the border of the functional ROI to reach a specific target volume, while preserving its original shape. Each ROI image (containing ones and zeros with ROI voxels having the value of one) was spatially smoothed in three dimensions using a 6-mm full-width-half-maximum isotropic kernel, then a series of thresholds were iteratively applied to this image until the target volume was reached. New voxels that appeared outside the cortex during this procedure were excluded (results in **Supplementary Fig. 1**).

Extraction of BOLD signals from ROIs. To measure BOLD signals, the raw time-course data was extracted from each ROI (see above). These data were then high-pass filtered (0.0052 Hz cutoff) and shifted in time by 3 s to account for hemodynamic lag. The average BOLD signals during each image condition and base line (fixation blocks) were estimated from the mean of the signal during each block after accounting for hemodynamic lag. The percent BOLD signal change for each image category was calculated relative to the average BOLD signal across fixation blocks:

$$100 \times \frac{(\text{category} - \text{fixation})}{\text{fixation}}$$

Estimation of factors associated with BOLD-related confounds. Results of these analyses are presented in **Supplementary Note 1** and **Supplementary Tables 1** and **2**.

1. Motion. The translational movement during the scan was calculated in millimeters ($d = \sum x^2, y^2, z^2)^{1/2}$ and the rotational motion in radians ($r = \sum \text{pitch, roll, yaw}$) based on the SPM2 parameters for motion correction of the functional images in each subject.

2. Fluctuation of BOLD responses during the fixation baseline – %cv_BOLD. We used this measure because it reflects fluctuations of the BOLD signal independently of the stimuli. %cv_BOLD was calculated per voxel as the coefficient of BOLD variation during fixation relative to the mean amplitude of the voxel across the entire time course and then averaged across the anatomical ROI:

$$\%cv_BOLD = 100 \times \frac{1}{N} \sum_{i=1}^N \frac{\sigma_i}{\mu_i}$$

where N is the number of voxels in the anatomical ROI, σ_i is the amplitude of noise fluctuations in a voxel during baseline and μ_i is the mean amplitude of the voxel's response. %cv_BOLD was calculated for the anatomical ROIs of the mFG bilaterally and the PHG bilaterally.

3. Residual error of GLM (%Res). This reflects the discrepancy between the GLM estimates and the time-course BOLD data, and thus is an inclusive measure of BOLD-related noise and goodness of GLM fit. The residual variance of the GLM was estimated per voxel using ResMS.img generated by SPM2 during model estimation. We then measured the mean residual error across anatomical ROIs:

$$\%Res = 100 \times \frac{\frac{1}{N} \sqrt{\sum_{i=1}^N \text{ResMs}(i)}}{\text{Mean Amp}}$$

where N is the number of voxels in the anatomical ROI and MeanAmp is the mean amplitude of the BOLD response across the ROI,

$$\text{MeanAmp} = \frac{1}{N} \sum_{i=1}^N \mu_i$$

The %Res was calculated across the anatomical ROIs of the mFG and the PHG (Supplementary Note 1). We then reanalyzed our data for subjects matched for BOLD-related confounds (details of matching procedure and results in Supplementary Note 1).

Experiment 2. Stimuli and data analysis. Outside the scanner, subjects participated in an independent recognition-memory task. During encoding, they viewed ten images (never seen before) of each of the categories including faces, abstract sculptures and scenes. All stimuli were gray-scale photographic images similarly prepared and presented as in Experiment 1. Subjects were instructed to perform a one-back task while viewing the images. Ten to 15 min later, during a self-paced subsequent recognition-memory test, subjects were presented with all the images from the encoding session plus an equal number (ten) of new images per category. Image categories and old and new pictures were randomly distributed during the session. Subjects were instructed to indicate whether they had seen the image before or not by pressing one of two buttons, as accurately and as quickly as possible. They were informed that none of the images were from the previous fMRI session. Performance accuracy and reaction times for the one-back task during encoding were calculated as described above. Accuracy for the subsequent recognition-memory task was calculated as $100 \times [\text{hits (old)} - \text{false alarms (new)}] / \text{number of old images}$, separately per image category and subject.

A *post hoc* analysis of recognition-memory performance per image—that is,

$$\frac{100}{N} \sum_{i=1}^N \text{correct responses}(i)$$

where $i = 1 - N$; N = number of subjects—showed that the percentage of correct responses per image was above 30% for adults and above 40% for children, suggesting that results were not driven by specific images that were particularly difficult to identify as old or new.

Statistical methods for between age-group comparisons. Subjects' data were averaged for each of the three age groups: 7–11-year-olds, 12–16-year-olds and adults. Between-group differences were evaluated by two-tailed ANOVA and *t*-tests, unless otherwise noted.

For between-group comparisons of the size of the functional or anatomically defined ROIs, we used one-way ANOVAs with the factor age. For between-group comparisons of the size of the functional ROIs, subjects who showed no activations fulfilling the definition of the particular functional ROI were assigned zero for the size of the ROI and included in the analysis. However, for between-group comparison of the percent BOLD signals within functionally defined ROIs, only subjects who showed activations fulfilling the definition of the functional ROI were included in the analysis. For between-group comparison of the number of voxels within the anatomical boundaries of the FFA or PPA, we used a GLM with the number of voxels as within-subject repeated measures. For between-group comparisons of responses (behavioral or BOLD signals) to the various image categories, we used a GLM with responses across categories as the within-subject repeated measures.

Note: Supplementary information is available on the Nature Neuroscience website.

ACKNOWLEDGMENTS

Thanks to A. Greenwood, G. Glover, P. Mazaika, C. Rorden and B. Wandell for useful suggestions, to S. Dean and L. Wood for help with scanning and behavioral tests, and to the participants in our experiments. This work was supported by US National Institutes of Health grants 5R21DA15893, 1R21MH66747, 1R21EY017741, T32 MH19908 and National Science Foundation grant BCS-0617688.

AUTHOR CONTRIBUTIONS

G.G., D.G.G., J.D.E.G. and K.G.-S. participated in all phases of this study. G.G. participated in designing the experiments, conducting fMRI and behavioral experiments, analyzing the data and preparing the manuscript. D.G.G. developed code for fMRI experiments and data analyses, helped with data collection and analysis and contributed to the manuscript. S.W.-G. contributed to code and data analyses. J.L.E. and A.R. contributed to the study design and the manuscript. K.G.-S. and J.D.E.G. supervised the study and contributed to experimental design, data collection and analysis, and the manuscript.

COMPETING INTERESTS STATEMENT

The authors declare no competing financial interests.

Published online at <http://www.nature.com/natureneuroscience>

Reprints and permissions information is available online at <http://npg.nature.com/reprintsandpermissions>

- Malach, R. *et al.* Object-related activity revealed by functional magnetic resonance imaging in human occipital cortex. *Proc. Natl. Acad. Sci. USA* **92**, 8135–8139 (1995).
- Kanwisher, N., McDermott, J. & Chun, M.M. The fusiform face area: a module in human extrastriate cortex specialized for face perception. *J. Neurosci.* **17**, 4302–4311 (1997).
- Tong, F., Nakayama, K., Vaughan, J.T. & Kanwisher, N. Binocular rivalry and visual awareness in human extrastriate cortex. *Neuron* **21**, 753–759 (1998).
- Grill-Spector, K., Knouf, N. & Kanwisher, N. The fusiform face area subserves face perception, not generic within-category identification. *Nat. Neurosci.* **7**, 555–562 (2004).
- Golby, A.J., Gabrieli, J.D.E., Chiao, J.Y. & Eberhardt, J.L. Differential responses in the fusiform region to same-race and other-race faces. *Nat. Neurosci.* **4**, 845–850 (2001).
- Nichols, E.A., Kao, Y.C., Verfaellie, M. & Gabrieli, J.D. Working memory and long-term memory for faces: evidence from fMRI and global amnesia for involvement of the medial temporal lobes. *Hippocampus* **16**, 604–616 (2006).
- Ranganath, C., DeGutis, J. & D'Esposito, M. Category-specific modulation of inferior temporal activity during working memory encoding and maintenance. *Brain Res. Cogn. Brain Res.* **20**, 37–45 (2004).
- Epstein, R. & Kanwisher, N. A cortical representation of the local visual environment. *Nature* **392**, 598–601 (1998).
- Stern, C.E. *et al.* The hippocampal formation participates in novel picture encoding: evidence from functional magnetic resonance imaging. *Proc. Natl. Acad. Sci. USA* **93**, 8660–8665 (1996).
- Brewer, J.B., Zhao, Z., Desmond, J.E., Glover, G.H. & Gabrieli, J.D. Making memories: brain activity that predicts how well visual experience will be remembered. *Science* **281**, 1185–1187 (1998).
- Kanwisher, N. Domain specificity in face perception. *Nat. Neurosci.* **3**, 759–763 (2000).
- Gauthier, I. What constrains the organization of the ventral temporal cortex? *Trends Cogn. Sci.* **4**, 1–2 (2000).

13. Tarr, M.J. & Gauthier, I. FFA: a flexible fusiform area for subordinate-level visual processing automatized by expertise. *Nat. Neurosci.* **3**, 764–769 (2000).
14. Haxby, J.V. *et al.* Distributed and overlapping representations of faces and objects in ventral temporal cortex. *Science* **293**, 2425–2430 (2001).
15. Goren, C.C., Sarty, M. & Wu, P.Y. Visual following and pattern discrimination of face-like stimuli by newborn infants. *Pediatrics* **56**, 544–549 (1975).
16. Johnson, M.H., Dziurawiec, S., Ellis, H. & Morton, J. Newborns' preferential tracking of face-like stimuli and its subsequent decline. *Cognition* **40**, 1–19 (1991).
17. de Haan, M. & Nelson, C.A. Brain activity differentiates face and object processing in 6-month-old infants. *Dev. Psychol.* **35**, 1113–1121 (1999).
18. Gauthier, I., Tarr, M.J., Anderson, A.W., Skudlarski, P. & Gore, J.C. Activation of the middle fusiform 'face area' increases with expertise in recognizing novel objects. *Nat. Neurosci.* **2**, 568–573 (1999).
19. Gauthier, I., Skudlarski, P., Gore, J.C. & Anderson, A.W. Expertise for cars and birds recruits brain areas involved in face recognition. *Nat. Neurosci.* **3**, 191–197 (2000).
20. Chance, J.E., Turner, A.L. & Goldstein, A.G. Development of differential recognition for own- and other-race faces. *J. Psychol.* **112**, 29–37 (1982).
21. Carey, S., Diamond, R. & Woods, B. The development of face recognition—a maturation component? *Dev. Psychol.* **16**, 257–269 (1980).
22. Jenkins, W.M., Merzenich, M.M. & Recanzone, G. Neocortical representational dynamics in adult primates: implications for neuropsychology. *Neuropsychologia* **28**, 573–584 (1990).
23. Haslinger, B. *et al.* Reduced recruitment of motor association areas during bimanual coordination in concert pianists. *Hum. Brain Mapp.* **22**, 206–215 (2004).
24. Tzourio-Mazoyer, N. *et al.* Neural correlates of woman face processing by 2-month-old infants. *Neuroimage* **15**, 454–461 (2002).
25. Gathers, A.D., Bhatt, R., Corbly, C.R., Farley, A.B. & Joseph, J.E. Developmental shifts in cortical loci for face and object recognition. *Neuroreport* **15**, 1549–1553 (2004).
26. Aylward, E.H. *et al.* Brain activation during face perception: evidence of a developmental change. *J. Cogn. Neurosci.* **17**, 308–319 (2005).
27. Huetzel, S.A., Singerman, J.D. & McCarthy, G. The effects of aging upon the hemodynamic response measured by functional MRI. *Neuroimage* **13**, 161–175 (2001).
28. Thomason, M.E., Burrows, B.E., Gabrieli, J.D. & Glover, G.H. Breath holding reveals differences in fMRI BOLD signal in children and adults. *Neuroimage* **25**, 824–837 (2005).
29. Weisberg, J., van Turenout, M. & Martin, A. A neural system for learning about object function. *Cereb. Cortex*, **17**, 513–521 (2007).
30. Downing, P.E., Jiang, Y., Shuman, M. & Kanwisher, N. A cortical area selective for visual processing of the human body. *Science* **293**, 2470–2473 (2001).
31. Kronbichler, M. *et al.* The visual word form area and the frequency with which words are encountered: evidence from a parametric fMRI study. *Neuroimage* **21**, 946–953 (2004).
32. Grill-Spector, K., Kushnir, T., Hendler, T. & Malach, R. The dynamics of object-selective activation correlate with recognition performance in humans. *Nat. Neurosci.* **3**, 837–843 (2000).
33. Grill-Spector, K., Sayres, R. & Ress, D. High-resolution imaging reveals highly selective nonface clusters in the fusiform face area. *Nat. Neurosci.* **9**, 1177–1185 (2006).
34. Kobatake, E., Wang, G. & Tanaka, K. Effects of shape-discrimination training on the selectivity of inferotemporal cells in adult monkeys. *J. Neurophysiol.* **80**, 324–330 (1998).
35. Dalton, K.M. *et al.* Gaze fixation and the neural circuitry of face processing in autism. *Nat. Neurosci.* **8**, 519–526 (2005).
36. Conner, I.P., Sharma, S., Lemieux, S.K. & Mendola, J.D. Retinotopic organization in children measured with fMRI. *J. Vis.* **4**, 509–523 (2004).
37. Yue, X., Tjan, B.S. & Biederman, I. What makes faces special? *Vision Res.* **46**, 3802–3811 (2006).
38. Anastasi, J.S. & Rhodes, M.G. An own-age bias in face recognition for children and older adults. *Psychon. Bull. Rev.* **12**, 1043–1047 (2005).
39. Gilbert, C. & Bakan, P. Visual asymmetry in perception of faces. *Neuropsychologia* **11**, 355–362 (1973).
40. De Renzi, E., Perani, D., Carlesimo, G.A., Silveri, M.C. & Fazio, F. Prosopagnosia can be associated with damage confined to the right hemisphere—an MRI and PET study and a review of the literature. *Neuropsychologia* **32**, 893–902 (1994).
41. Rossion, B. *et al.* Hemispheric asymmetries for whole-based and part-based face processing in the human fusiform gyrus. *J. Cogn. Neurosci.* **12**, 793–802 (2000).
42. Allison, T., Puce, A. & McCarthy, G. Social perception from visual cues: role of the STS region. *Trends Cogn. Sci.* **4**, 267–278 (2000).
43. Epstein, R.A., Higgins, J.S., Parker, W., Aguirre, G.K. & Cooperman, S. Cortical correlates of face and scene inversion: a comparison. *Neuropsychologia* **44**, 1145–1158 (2006).
44. Yovel, G. & Kanwisher, N. Face perception: domain specific, not process specific. *Neuron* **44**, 889–898 (2004).
45. Grill-Spector, K. *et al.* A sequence of object-processing stages revealed by fMRI in the human occipital lobe. *Hum. Brain Mapp.* **6**, 316–328 (1998).
46. Lerner, Y., Hendler, T., Ben-Bashat, D., Harel, M. & Malach, R. A hierarchical axis of object processing stages in the human visual cortex. *Cereb. Cortex* **11**, 287–297 (2001).
47. Grill-Spector, K. The neural basis of object perception. *Curr. Opin. Neurobiol.* **13**, 159–166 (2003).
48. Glover, G.H. & Law, C.S. Spiral-in/out BOLD fMRI for increased SNR and reduced susceptibility artifacts. *Magn. Reson. Med.* **46**, 515–522 (2001).
49. Smith, S.M. Fast robust automated brain extraction. *Hum. Brain Mapp.* **17**, 143–155 (2002).
50. Duvernoy, H. *The Human Brain* (Springer, Wien and New York, 1999).